Nanoscale squeezing in elastomeric nanochannels for single chromatin linearization

*Toshiki Matsuoka[1], Byoung Choul Kim[1‡], Jiexi Huang[2‡], Nicholas Douville[1‡], M.D. Thouless[2,3] and Shuichi Takayama[1,4]**

[1]Department of Biomedical Engineering, College of Engineering, University of Michigan, 2800 Plymouth Rd, Ann Arbor, MI 48109, USA

[2]Department of Mechanical Engineering, College of Engineering, University of Michigan, 2350 Hayward St., Ann Arbor, MI 48109, USA

[3]Department of Materials Science & Engineering, College of Engineering, University of Michigan, 2300 Hayward St., Ann Arbor, MI 48109, USA

[4]Division of Nano-Bio and Chemical Engineering WCU Project, UNIST, Ulsan, Republic of Korea

ABSTRACT: This paper describes a novel nanofluidic phenomenon where untethered DNA and chromatin are linearized by rapidly narrowing an elastomeric nanochannel filled with solutions of the biopolymers. This nanoscale squeezing procedure generates hydrodynamic flows while also confining the biopolymers into smaller and smaller volumes. The unique features of this technique enable full linearization then trapping of biopolymers such as DNA. The versatility of the method is also demonstrated by analysis of chromatin stretchability and mapping of histone states using single strands of chromatin.

KEYWORDS: nanochannel, nanoconfinement, biopolymer, epigenetics

An important purpose of micro- and nanofluidics research is to develop new types of fluid flows useful for biomolecular analysis.[1-10] Here, we report the generation of a mixed shear and elongational flow by collapsing fluid-filled elastomeric sub-micron channels to the molecular scale. The potential of this nanoscale squeezing technique is first demonstrated by stretching lambda DNA to its full contour length in physiological buffers and trapping it in that state. Additionally, we demonstrate the ability to distinguish the difference in stretchability between chromatin reconstituted with and without histone H1, as well as the ability to simultaneously map histone acetylation and methylation states from single strands of chromatin.

The quest for highly stretched DNA, especially if it can be immobilized in that state, is not only a scientific interest but a goal with practical implications as well. For example, optical mapping of DNA would benefit from highly stretched, immobilized DNA because it would reduce uncertainties in the correlations between visually measured lengths (nanometers) versus genomic lengths (basepairs) and reduce effects of thermal fluctuations. Several previous papers report "full" elongation of DNA by flow[11] or nanoconfinement[12]; however the degree of elongation reported in these papers is limited to ~90% of the contour length. These earlier procedures also used either non-physiological buffers that lack salts[12] or high-viscosity solutions to increase the shear stress.[11] These extreme conditions for the solutions are not only inconvenient, but can preclude handling of delicate biopolymers such as chromatin where physiological buffers are a prerequisite to maintain the higher-order structures.[13-15] The inherent conflict between the requirement for very narrow channels to achieve a high degree of linearization and the requirement for sufficiently wide channels to introduce large-radius biopolymers efficiently is also difficult to overcome. Finally, chromatin linearization is even more complex than DNA linearization because chromatin flexibility and, hence, persistence

length is not constant, but depends on histone modifications[16,17] and the presence or absence of irregularly folded nucleosome fibers.[18] In other words, the ideal nanochannel size for chromatin linearization relying on nanoconfinement alone is variable. Channels that are too narrow may preclude certain chromatin regions from entering the nanochannels or force loss of structural proteins as a consequence of forced introduction. Channels that are too wide would lead to incomplete linearization. The nanoscale squeezing method described here (Figure 1a) overcomes all of these limitations of conventional nanochannels by gradually narrowing a size-adjustable nanochannel. Not only does this solve the problem of easy biopolymer loading, the hydrodynamic flows enable extensive linearization of the biopolymers.

In this procedure, an elastomeric poly(dimethylsiloxane) (PDMS) slab with two parallel reservoirs is bonded using plasma oxidation with a thin PDMS film (Supporting Information, Figure 1). The PDMS structure is stretched in a direction parallel to the direction of the reservoirs. This results in the spontaneous formation of an array of tunneling cracks, connecting the two reservoirs.[19] Electrical-impedance methods showed that the average cross-sectional area of these channels at 10% strain, considered the fully-opened state, was ~15000 nm^2 (Supporting Information, Figure 2). This cross-sectional area is sufficient to allow the efficient loading of large-radius coiled DNA and chromatin into the channels. When the strain is subsequently relaxed, the channel cross-sectional dimensions decrease significantly (Supporting Information, Figure 2b). This narrowing linearizes and traps these biopolymers in an extended state. For example, when the channels were closed from 10% to 1% strain in a series of quick (0.5 s) steps, λ-DNA became extended up to 97% of its contour length (Figure 1b). This result was obtained without the application of an electric field, and was verified by using YOYO-1 stained DNA (4 base pair/1 dye molecule) that had both ends labeled with additional fluorescent markers. The

ability to stably trap the linearized DNA, rather than have it moving or flowing, enabled high-resolution visual pinpointing of the single molecule fluorescent labels at the DNA ends. It should be noted that while our labs previously reported on crack-induced nanochannels,[19,20] the DNA elongation in those studies was obtained using nanoconfinement in conjunction with an electrophoretic driving force.[18] The degree of linearization achieved previously was also much less (60% vs 97%) and in a regime where the stiffness of the DNA, estimated as an unconfined worm-like polymer, would be over two orders of magnitude smaller.[21,22] The concept of inducing mixed elongational and shear flows by relaxation of an applied tensile strain to reduce the cross-sectional dimensions of channels and its potential to achieve nearly full linearization of DNA, without an electric field or imposed external pressure gradient, was not recognized.

Nanoscale squeezing can also reveal stretchability differences in chromatin reconstituted with and without histone H1 (Figure 1c).[23-25] These results indicate that while the linearization conditions can be sufficiently vigorous to allow full linearization of DNA, the procedure can also be gentle enough and compatible with physiological buffers to maintain higher-order structures of chromatin. The variability in length distribution for each type of chromatin reflects a combination of nanochannel heterogeneity as well as heterogeneities in the original samples (e.g. lambda DNA fragments and dimers, and partial reconstitution of chromatin).[26,27]

We hypothesize that the elongation of the biopolymers comes from the unique combination of hydrodynamic flows and nanoconfinement generated during the closing of the nanochannels. An asymptotic analysis shows that narrowing the long and thin crack-induced channels produce flows with combined elongational and shear components. We estimate an accumulated strain (Hencky strain) of up to ~8 along the centerline of the channel assuming a residency time of 0.5 s during each of the four steps (Figure 2a and Supporting Information, Table 1), and assuming

that the strain accumulates among steps. These are of a similar order of magnitude to the strains reported by Perkins *et al.* required to achieve ~80% extension of λ-DNA using purely elongational flows.[2] We note, however, that the stiffness of the DNA in solution would be ~40 times higher at the 97% extension compared to the previously reported 80%. Nanoscale squeezing combines moderately high shear rates of 8000-20000 s^{-1} with nanoconfinement that decreases entropic freedom as well as increases the DNA relaxation time from 60 ms in the bulk to a few seconds leading to high Weissenberg number (*Wi*) (Figure 2b and Supporting Information, Table 1).[2,3] Additionally, nanoconfinement maintains the orientation of the DNA with respect to the shear direction, even though the flow contains rotational components.[27] These factors combine to enable hydrodynamic DNA linearization to levels beyond typical limits of 80%. Finally, narrowed nanochannels trap the DNA molecules in their linearized state once the transiently generated squeezing flows terminate.

In linearization experiments, we found two procedural aspects critical to the efficiency of linearization. First, rapid relaxation of the applied tensile strain, which results in higher rates of elongational shear flows, is more efficient than slower narrowing of the channels. Second, relaxation of the applied tensile strain in a series of rapid increments with a brief hold between them gives higher yields of linearized DNA than completely collapsing the nanochannel in a single step. While the single step can produce higher rates of elongational shear flows, it produces more nanochannel bubbles where the channel collapses before the fluid has been completely flushed out, leaving local pockets of large cross-sectional areas (Supporting Information, Figure 3). Analysis of the velocity of quantum dots during nanoscale squeezing show that flow velocities reach at least 40 μm/s using a multi-step quick narrowing procedure; slower relaxation resulted in velocities that were an order of magnitude less (Figure 2c-d). It

should be noted that fluid flows with DNA molecules may be even faster than those measured using quantum dots, because of the relatively large size of the quantum dots (diameter ~ 20 nm) with respect to the width of the channels. Indeed, calculations estimate fluid velocities to be as high as 300 μm/s.

The observed distribution of DNA conformations obtained by the nanoscale squeezing procedure (Figure 2e-f and Supporting Information, Figure 4) is consistent with the notion that the linearization process is hydrodynamically driven. Specifically, increased observations of the highly-extended DNA conformations are accompanied by the reduced occurrence of the stretched dumbbell conformations.[2] This shift is evident in comparison both to previously reported hydrodynamic DNA stretching experiments[2] and to nanoscale squeezing procedures that have incomplete nanochannel closure (Supporting Information, Figure 5). The existence of minimally extended DNA even with full channel closure is again a consequence of nanochannel bubbles that leave local large cross-sectional areas pockets. Some DNA may also be trapped in metastable conformations (Supporting Information, Figure 5).

Broader utility of the nanoscale squeezing procedure was explored by linearizing and performing multi-color imaging of single strands of chromatin (Figure 3 and Supporting Information, Figure 6). The chromatin in figure 3a, isolated from HeLa cells, was stained with DAPI (stains DNA blue) and two antibodies against methylated histone H3 (labels methylated histone H3K9me3 green) and acetylated histone H4 (labels acetylated histone H4 red) prior to linearization. The H3K9me3 marks co-localized mainly with higher DNA stained regions consistent with its role in highly condensed chromatin such as heterochromatin.[16,17] The chromatin in figure 3b (see also Supporting Information, Figure 7), was isolated from GFP-histone (stains most nucleosomes green) expressing cells and further labeled with DAPI (blue)

and an antibody against acetylated histone H4 (red) prior to linearization. Image analysis of this linearized chromatin reveals positions of chromatin condensation and different histone modifications over an extended genomic region.

In this study, we demonstrated a novel, nanoscale squeezing procedure that can linearize DNA and chromatin and trap the linearized biopolymers in physiological buffers (Figure 1). The extent of linearization (>95%) achieved is unprecedented for DNA, let alone achieving it in physiological buffers. Analysis of the changes in distribution of DNA conformations supports the notion that the biopolymer linearization process of nanoscale squeezing involves a significant hydrodynamic element (Figure 2). We further demonstrated linearization, trapping, and multi-color histone state analysis of linearized and trapped chromatin (Figure 3). While chromatin immunoprecipitation (ChIP) assays are commonly used for histone state mapping, ChIP assays do have weaknesses. For example, histone state mapping is difficult in regions with many repeat sequences such as retrotransposon. ChIP based methods also only allow analysis of one epigenetic marker from each sample. Thus, ChIP-based chromatin mapping is difficult when sample is scarce as in the case of rare cell analysis. As chromatin cannot be amplified the way DNA can be, development of single chromatin analysis capabilities will be critical for advancing epigenetic studies.[29,30]

The squeezing channels used were prepared by cracking, a method that is physically interesting and attractive for its convenience, speed, and low cost. In current experiments, one 1 cm^2 device with an array of ~700 nanochannels (300 μm long nanochannels) yielded 70 linearized chromatin fragments of various lengths (Supporting Information, Figure 8) totaling ~20 Mb. The devices and procedures can be readily scaled up to much larger areas and chromatin linearization capacities. Finally, although this paper focuses on DNA and chromatin

linearization using fracture-fabricated nanochannels, nanoscale squeezing is a general nanofluidic concept that should find applications in areas beyond biopolymer linearization and to channel types made by methods other than cracking as well.

FIGURES

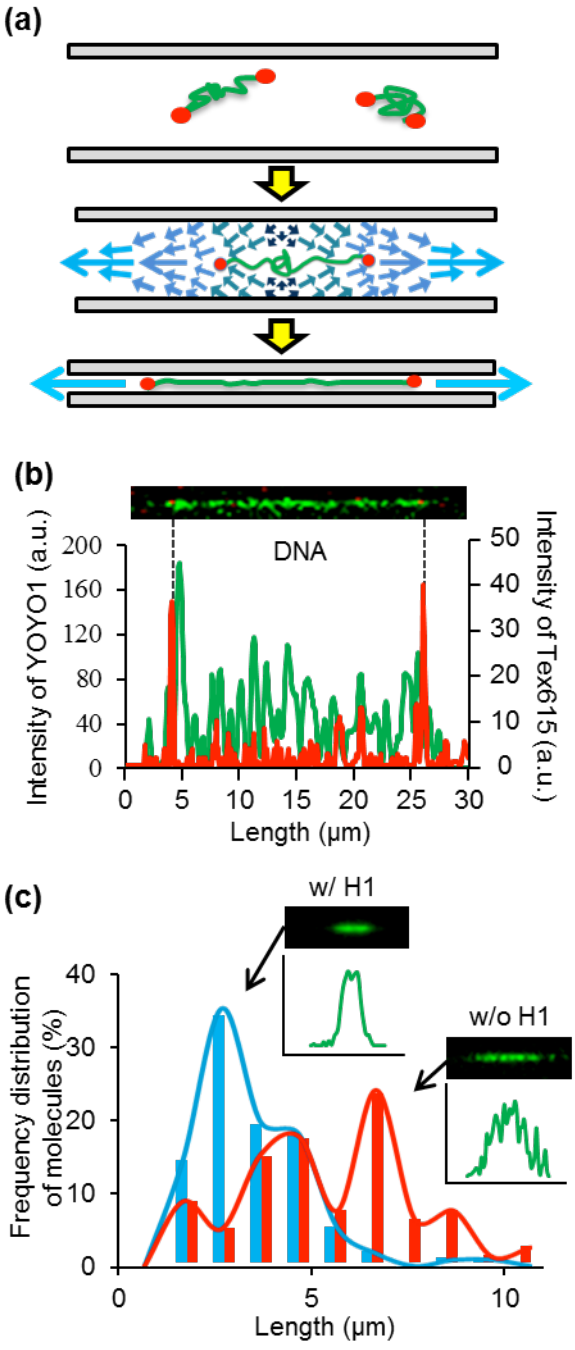

Figure 1. DNA linearization by nanoscale squeezing. (a) Nanoscale squeeze flow and nanoconfinement induce linearization of biopolymers. (b) An example of a fluorescence image and intensities of a 97% linearized λ-DNA. The graph shows the intensities of YOYO-1 (green) and TEX615 (red) labels at the DNA ends (a.u. = arbitrary unit). (c) A plot of the frequency distribution of the lengths of linearized reconstituted chromatin prepared from λ-DNA with histone H1 (blue) and without histone H1 (red). Insets show fluorescence images of the linearized reconstituted chromatin with or without histone H1. The graphs under each images show YOYO-1 intensity, respectively.

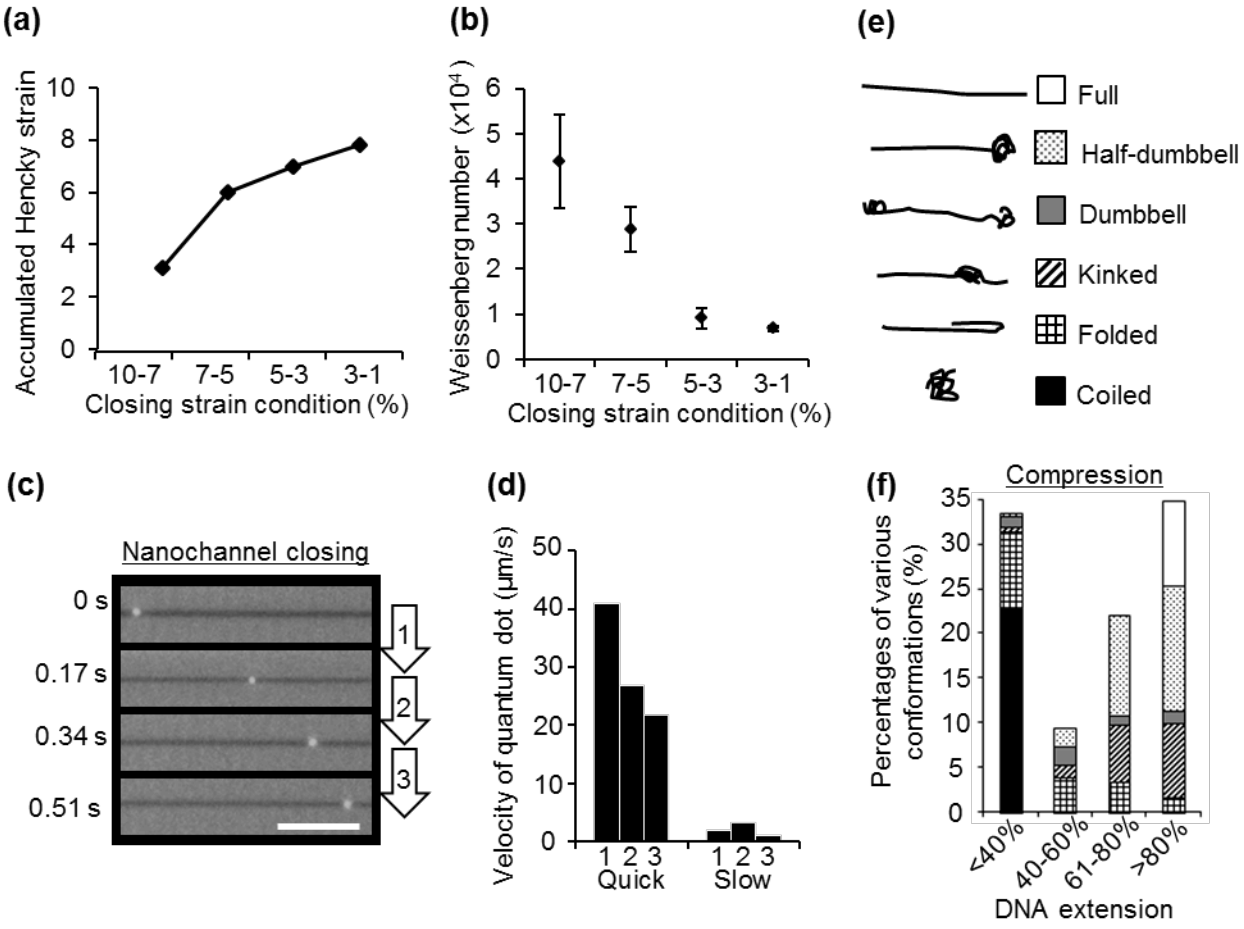

Figure 2. Nanoscale squeezing generates vigorous flow conditions that hydrodynamically linearize biopolymers. (a) Estimated accumulated Hencky strain as the applied strain is relaxed from 10% to 7%, 7% to 5%, 5% to 3% and 3% to 1%, respectively (Supporting Information, Table 1). (b) Estimated Weissenberg numbers (*Wi*) as applied strain is relaxed from 10% to 7%, 7% to 5%, 5% to 3% and 3% to 1%, respectively (Supporting Information, Table 1). (c) A quantum dot moving due to squeezing flows generated when strain is quickly relaxed from an initial value of 10% to 7%. Scale bar is 5 μm. (d) Measured velocity of quantum dots during the first 0.5 s as strain applied to the channels is relaxed from 10% to 7% strain using a quick (0.5 s) or slow (5.0 s) strain-release procedure. Numbers on the x-axis correspond to numbers on the arrows in Figure 2c. These arrows represent each 0.17 s period of observation. (e) Schematic drawing of various conformations of DNA. (f) Distribution of DNA conformations according to their degree of linearization as observed after performing stepwise nanoscale squeezing from 10% to 7% to 5% to 3% to −0.5% (Supporting Information, Table 2). DNA linearized to over 95% of the contour length was considered as being fully stretched.

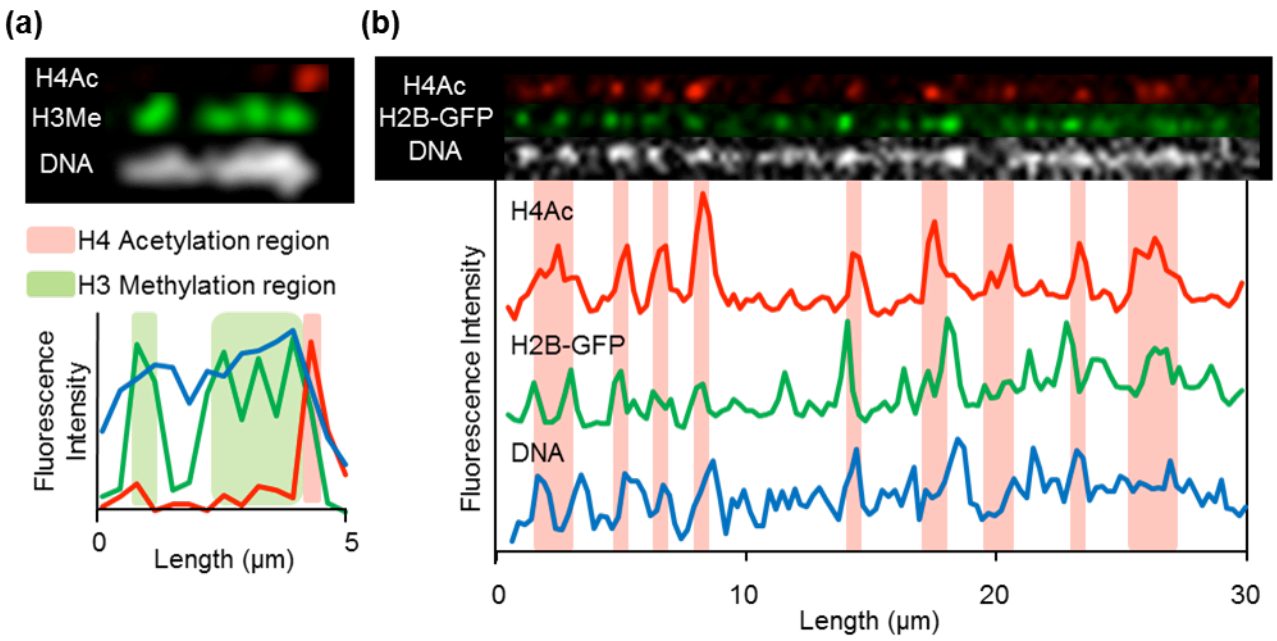

Figure 3. Chromatin linearization by nanoscale squeezing. (a) Linearization of chromatin isolated from HeLa cell. The DNA is stained with DAPI (white). Acetylated Histone H4 (H4Ac) is stained with labeled anti-H4Ac antibody (red). Methylated Histone H3K9 (H3Me) is stained with labeled anti-H3K9me3 antibody (green). (b) Linearization of chromatin isolated from HeLa cell expressing histone H2B-GFP (green). The DNA is stained with DAPI (white). Acetylated Histone H4 (H4Ac) is stained with labeled anti-H4Ac antibody (red). The acetylated histone regions are distinguished by the degree of H4Ac staining on the graph.

Supporting Information

Experimental details, additional device characterization and estimation of Weissenberg number and Hencky strain. This material is available free of charge via the Internet at http://pubs.acs.org.

AUTHOR INFORMATION

Corresponding Author

*E-mail: (S.T.) takayama@umich.edu; (M.D.T.) thouless@umich.edu

Author Contributions

The manuscript was written through contributions of all authors. All authors have given approval to the final version of the manuscript. ‡These authors contributed equally.

Funding Sources

This work was supported by a grant from the US National Institutes of Health (HG004653-03).

Notes

Any additional relevant notes should be placed here.

ACKNOWLEDGMENT

We thank Prof. RH. Austin, RG. Larson, W.W. Schultz, M. Burns, D. Burke, J. Biteen and T. Glover for comments on the project. We thank H. Kimura for kindly providing the HeLa cell Histone-GFP expressing cell line. This work was supported by a grant from the US National Institutes of Health (HG004653-03).

ABBREVIATIONS

DAPI, 4',6-Diamidino-2-Phenylindole, Dihydrochloride; ChIP, Chromatin immunoprecipitation; GFP, Green fluorescence protein; H4Ac, Acetylated Histone H4; H3Me, Methylated Histone H3; PDMS, polydimethylsiloxane; Wi, Weissenberg number.

REFERENCES

(1) Perkins, T. T.; Smith, D. E.; Larson, R. G.; Chu, S. *Science* **1995,** 268, 83-7.

(2) Perkins, T. T.; Smith, D. E.; Chu, S. *Science* **1997,** 276, 2016-21.

(3) Reisner, W.; Morton, K. J.; Riehn, R.; Wang, Y. M.; Yu, Z.; Rosen, M.; Sturm, J. C.; Chou, S. Y.; Frey, E.; Austin, R. H. *Phys. Rev. Lett.* **2005,** 94, 196101.

(4) Cipriany, B. R.; Zhao, R.; Murphy, P. J.; Levy, S. L.; Tan, C. P.; Craighead, H. G.; Soloway, P. D. *Anal. Chem.* **2010,** 82, 2480-7.

(5) Cipriany, B. R.; Murphy, P. J.; Hagarman, J. A.; Cerf, A.; Latulippe, D.; Levy, S. L.; Benitez, J. J.; Tan, C. P.; Topolancik, J.; Soloway, P. D.; Craighead, H. G. *Proc. Natl. Acad. Sci. U S A* **2012,** 109, 8477-82.

(6) Lam, E. T.; Hastie, A.; Lin, C.; Ehrlich, D.; Das, S. K.; Austin, M. D.; Deshpande, P.; Cao, H.; Nagarajan, N.; Xiao, M.; Kwok, P. Y. *Nat. biotechnol.* **2012**, 30, 771- 6.

(7) Reisner, W.; Pedersen, N. J.; Austin, H. R. *Rep. Prog. Phys.* **2012,** 106601.

(8) Persson, F.; Tegenfeldt, O. J. *Chem. Soc. Rev.* **2010,** 39, 985-99.

(9) Douville, N.; Huh, D.; Takayama, S. *Anal. Bioanal. Chem.* **2008,** 391, 2395-409.

(10) Chantiwas, R.; Park, S.; Soper, A. S.; Kim, BC.; Takayama, S.; Sunkara, V.; Hwang, H.; Cho, Y.-K. *Chem. Soc. Rev.* **2011,** 40, 3677-702.

(11) Perkins, T. T.; Quake, S. R.; Smith, D. E.; Chu, S. *Science* **1994,** 264, 822-6.

(12) Kim, Y.; Kim, K. S.; Kounovsky, K. L.; Chang, R.; Jung, G. Y.; dePablo, J. J.; Jo, K.; Schwartz, D. C. *Lab Chip* **2011,** 11, 1721-9.

(13) Campbell, A. M.; Cotter, R. I.; Pardon, J. F. *Nucleic Acids Res.* **1978,** 5, 1571-80.

(14) Suau, P.; Bradbury, E. M.; Baldwin, J. P. *Eur. J. Biochem.* **1979,** 97, 593-602.

(15) Woodcock, L. C.; Ghosh, P. R. *Cold Spring Harb. Rerspect. Biol.* **2010,** 2, a000596.

(16) Tamaru, H. *Genes. Dev.* **2010,** 24, 1465-78.

(17) Fierz, B.; Muir, T. W. *Nat.chem. biol.* **2012,** 8, 417-27.

(18) Nishino, Y.; Eltsov, M.; Joti, Y.; Ito, K.; Takata, H.; Takahashi, Y.; Hihara, S.; Frangakis, A. S.; Imamoto, N.; Ishikawa, T.; Maeshima, K. *EMBO J.* **2012,** 31, 1644-53.

(19) Mills, K. L.; Huh, D.; Takayama, S.; Thouless, M. D. *Lab Chip* **2010,** 10, 1627-30.

(20) Huh, D.; Mills, K. L.; Zhu, X.; Burns, M. A.; Thouless, M. D.; Takayama, S. *Nat. Mater.* **2007,** 6, 424-8.

(21) Bustamante, C.; Marko, J. F.; Siggia, E. D.; Smith, S. *Science* **1994,** 265, 1599-600.

(22) Marko, J. F.; Siggia, E. D. *Macromolecules* **1995,** 28, 8759-8770.

(23) Collepardo-Guevara, R.; Schlick, T. *Nucl. Acid Res.* **2012,** 1-15.

(24) Collepardo-Guevara, R.; Schlick, T. *Biophys. J.* **2011,** 101, 1670-80.

(25) Xiao, B.; Freedman, S. B.; Miller, E. K.; Heald, R.; Marko, F. J. *Mol. Biol. Cell* **2012,** doi:10/1091.

(26) Schlick, T.; Hayes, J.; Grigoryev, S. *J. Biol. Chem.* **2012,** 287, 5183-91.

(27) Streng, D. E.; Lim, S. F.; Pan, J.; Karpusenka, A.; Riehn, R. *Lab Chip* **2009,** 9, 2772-4

(28) Smith, D. E.; Babcock, H. P.; Chu, S. *Science* **1999,** 283, 1724-7.

(29) Rasmussen, K. H.; Marie, R.; Lange, J. M.; Svendsen, W. E.; Kristensen, A.; Mir, K. U. *Lab Chip* **2011,** 11, 1431-3.

(30) Cerf, A.; Tian, C. H.; Craighead, G. H. *Acs Nano* **2012,** 6, 7928-34.